

Design of an Advanced Atomic Force Microscope Control Electronics using FPGA

by  
İhsan Kehribar  
2013

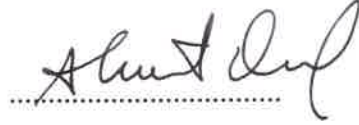
Submitted to the Graduate School of Engineering and Natural Sciences  
in partial fulfillment of  
the requirements for the degree of  
Master of Science

Sabanci University  
January 2013

DESIGN OF AN ADVANCED ATOMIC FORCE MICROSCOPE  
ELECTRONICS USING FPGA

APPROVED BY:

Prof. Dr. Ahmet Oral  
(Thesis Advisor)



Assoc. Prof. ErKay Savaş



Assoc. Prof. Ayhan Bozkurt



Assoc. Prof. H. Özgür Özer



Assoc. Prof. İsmet İnönü Kaya



DATE OF APPROVAL: 28.01.2013

© Ihsan Kehribar 2013  
All Rights Reserved

*to my family & my fiancée Ebru*



## **Acknowledgments**

I would like to thank my supervisor, Prof. Dr. Ahmet Oral for his continuous support and encouragement throughout this thesis. It was a very unique experience to work with him and I certainly learned a lot during the process.

I am very thankful to my thesis committee members İsmet İnönü Kaya, Ayhan Bozkurt, H. Özgür Özer and Erkay Savaş for their valuable comments and suggestions on this thesis.

I especially thank to Ümit Çelik for his valuable technical and social support in broad range of subjects during my research.

I would like to thank my roommate Mustafa Yalçın for his friendship and support.

I would like to thank to members of Scanning Probe Microscopy & Nanomagnetism Laboratory for their friendship and support during my studies. I especially would like to thank to Süleyman Çelik for his company and technical support during my late hour research and development sessions.

I am grateful to Tübitak and SANTEZ program for providing financial support during my studies.

I also would like to thank to employers of Nanomagnetism Instruments, especially to Erşan Tunçkol, Burhan Eyimaya and Celil Tanrıkkurt for their contributions in technical development of my thesis.

Finally, I would like to express my special appreciation to my family for their unconditional love and support.

# DESIGN OF AN ADVANCED ATOMIC FORCE MICROSCOPE CONTROL ELECTRONICS USING FPGA

İhsan Kehribar

Ms Thesis, 2013

Thesis Supervisor: Prof. Dr. Ahmet Oral

Keywords: Atomic Force Microscopy, FPGA

## ABSTRACT

Atomic Force Microscope (AFM) is a great scientific and R&D tool. AFM can obtain 3D surface topography of objects with atomic resolution. AFM can provide images of conductive, non-conductive and also biological samples. Invention of the AFM led to many improvements in the several areas like material science, physics and biology. Additionally, AFM has a wide range of applications like the quality control and production testing in the industry. In spite of AFM's many advantages and specialties, price and the complexity of the available AFM options makes it harder for researchers and companies to reach this technology.

To address this issue, easy to use Atomic Force Microscope ezAFM is designed with joint efforts of Sabanci University - "Scanning Probe Microscopy & Nanomagnetism Laboratory", Istanbul Technical University - "Nanomechanics Laboratory" and NanoMagnetics Instruments & NanoSis and with the support of "Ministry of Science, Industry and Technology", through the SANTEZ program. The ezAFM is a user friendly, compact and high performance novel AFM system. The ezAFM is very affordable and similar to a lab grade optical microscope.

In this thesis, the Control Electronics design and the PC software architecture of the ezAFM will be discussed.

# GELİŞMİŞ BİR ATOMİK KUVVET MİKROSKOBU KONTROL ELEKTRONİĞİNİN FPGA KULLANILARAK TASARLANMASI

İhsan Kehribar

Ms Tezi, 2013

Tez Danışmanı: Prof. Dr. Ahmet Oral

Anahtar Kelimeler: Atomik Kuvvet Mikroskobu, FPGA

## ÖZET

Atomik Kuvvet Mikroskobu (AKM) bilimsel ve araştırma-geliştirme amaçlarında kullanılan çok önemli bir araçtır. AKM incelediği örneklerin atomik çözünürlükte 3 boyutlu yüzey haritalarını çıkarabilir. AKM iletken, yalıtkan veya biyolojik özellikteki örnekleri tarayabilir. AKM'nin icadı fizik, biyoloji ve malzeme bilimi gibi alanlarda bir çok gelişmelere yol açmıştır. Bilim alanına ek olarak AKM'nin endüstride de kalite kontrolü ve üretim testi gibi alanlarında çok geniş uygulama alanları mevcuttur. AKM'nin bütün bu avantaj ve özelliklerine rağmen piyasadaki mevcut AKM'lerin fiyatları ve kompleksiteleri şirketlerin ve araştırmacıların bu teknolojiye ulaşabilmesini zorlaştırmaktadır.

Bu duruma çözüm bulmak için kolay kullanılabilir Atomik Kuvvet Mikroskobu ezAFM, Sabancı Üniversitesi Taramalı Uç Mikroskopları ve Nanomanyetizma Labaratuvarı, İstanbul Teknik Üniversitesi Nanomekanik Labaratuvarı ve NanoMagnetics Instruments & NanoSis'in ortak çabaları ve SANTEZ programı üzerinden Endüstri ve Sanayi Bakanlığının desteğiyle tasarlandı. ezAFM kullanıcı dostu kompakt ve yüksek performanslı yenilikçi bir AKM sistemidir. ezAFM erişilebilirlik açısından oldukça uygundur ve labaroutaver seviyesi bir optik mikroskopa benzerdir.

Bu tez içerisinde ezAFM'in kontrol elektroniği ve PC yazılım altyapısı tartışılmaktadır.

## TABLE OF CONTENTS

<b>1</b>	<b>INTRODUCTION</b> .....	<b>1</b>
<b>1.1</b>	<b>Motivation</b> .....	<b>1</b>
<b>1.2</b>	<b>Outline of the Thesis</b> .....	<b>1</b>
<b>2</b>	<b>BACKGROUND AND RELATED WORKS</b> .....	<b>2</b>
<b>2.1</b>	<b>Historical Background</b> .....	<b>2</b>
2.2	Atomic Force Microscopy .....	5
2.2.1	Contact Mode Atomic Force Microscopy .....	5
2.2.2	Friction Force Microscopy .....	6
2.2.3	Tapping Mode Atomic Force Microscopy .....	6
<b>2.3</b>	<b>The Forces Measured by AFM</b> .....	<b>7</b>
<b>2.4</b>	<b>Deflection Measurement of AFM cantilever</b> .....	<b>8</b>
2.4.1	Tunneling Sensor .....	8
2.4.2	Optical Beam Deflection .....	8
2.4.3	Piezoresistive Cantilever .....	8
<b>2.5</b>	<b>The Scanners Used in AFM</b> .....	<b>9</b>
2.5.1	Piezo Tube Scanners .....	9
2.5.2	Piezo Stack Scanners .....	9
2.5.3	Voice Coil Scanners .....	9
<b>2.6</b>	<b>Related Works</b> .....	<b>10</b>
<b>3</b>	<b>IMPLEMENTATION</b> .....	<b>11</b>
<b>3.1</b>	<b>FPGA and Embedded Software Architecture</b> .....	<b>11</b>
<b>3.1.1</b>	<b>FPGA Design</b> .....	<b>11</b>
<b>3.1.2</b>	<b>Microblaze CPU</b> .....	<b>11</b>
<b>3.1.3</b>	<b>Dual CPU Design</b> .....	<b>12</b>
<b>3.1.4</b>	<b>Custom Peripheral Core Implementation</b> .....	<b>12</b>
<b>3.2</b>	<b>Embedded Software Design</b> .....	<b>13</b>
<b>3.3</b>	<b>Data Acquisition</b> .....	<b>13</b>
<b>3.4</b>	<b>Voice Coil Scanner Design</b> .....	<b>13</b>
<b>3.4.1</b>	<b>Driver Mechanism</b> .....	<b>15</b>
<b>3.4.2</b>	<b>Advantages Over Piezoelectric Scanners</b> .....	<b>15</b>
<b>3.5</b>	<b>Cantilever Excitation</b> .....	<b>15</b>
<b>3.5.1</b>	<b>Excitation Frequency Tuning</b> .....	<b>16</b>
<b>3.5.2</b>	<b>Direct Digital Synthesizer (DDS)</b> .....	<b>17</b>
<b>3.6</b>	<b>Cantilever Deflection Measurement System</b> .....	<b>18</b>
<b>3.6.1</b>	<b>Constant Power Laser Driver</b> .....	<b>18</b>

<b>3.6.2</b>	<b>Quadrant Photodiode Readout.....</b>	<b>20</b>
3.6.3	Digital Lock-in Amplifier (LIA) Implementation .....	21
3.6.3.1	Mathematical Background of Lock-in Amplifier .....	22
3.6.3.2	Digital Implementation .....	24
<b>3.7</b>	<b>Coarse Approach Mechanism.....</b>	<b>24</b>
<b>3.8</b>	<b>Feedback Control System Design .....</b>	<b>25</b>
3.8.1	Digital Feedback Algorithm.....	26
3.8.2	Implementation Details .....	27
<b>3.9</b>	<b>PC Software Design .....</b>	<b>27</b>
<b>3.10</b>	<b>Communication Hardware Details .....</b>	<b>28</b>
<b>3.11</b>	<b>Communication Architecture .....</b>	<b>28</b>
<b>3.12</b>	<b>Task Assignment Approach.....</b>	<b>29</b>
<b>4</b>	<b>RESULTS AND CONCLUSION .....</b>	<b>31</b>
<b>4.1</b>	<b>Prototypes .....</b>	<b>31</b>
<b>4.2</b>	<b>Images .....</b>	<b>33</b>
<b>4.3</b>	<b>Publicity .....</b>	<b>37</b>
<b>4.4</b>	<b>Conclusion.....</b>	<b>39</b>
<b>5</b>	<b>BIBLIOGRAHPY .....</b>	<b>41</b>

## TABLE OF FIGURES

<b>Figure 2.1:</b> Atomic resolution surface image of Si(111)(7x7) .....	<b>3</b>
<b>Figure 2.2:</b> Basic Block Diagram of Scanning Tunneling Microscopy .....	<b>4</b>
<b>Figure 2.3:</b> Basic Block Diagram of an Atomic Force Microcopy System .....	<b>5</b>
<b>Figure 2.4:</b> Friction Force Microscopy Principle .....	<b>6</b>
<b>Figure 2.5:</b> Force Distance Curve of AFM Tip .....	<b>7</b>
<b>Figure 3.1:</b> Microblaze CPU.....	<b>12</b>
<b>Figure 3.2:</b> Operating Principle of Voice Coil Actuator .....	<b>14</b>
<b>Figure 3.3:</b> Block Diagram of Voice Coil Scanner Electronics .....	<b>15</b>
<b>Figure 3.4:</b> Block Diagram of Cantilever Excitation System .....	<b>16</b>
<b>Figure 3.5:</b> Phase and Frequency Response of a Cantilever .....	<b>16</b>
<b>Figure 3.6:</b> Block Diagram of a Simple DDS Module .....	<b>17</b>
<b>Figure 3.7:</b> Laser Beam Deflection Measurement.....	<b>18</b>
<b>Figure 3.8:</b> Output Power – Forward Current Graph of a Laser Diode.....	<b>19</b>
<b>Figure 3.9:</b> Monitor Current – Output Power Graph of a Laser Diode .....	<b>19</b>
<b>Figure 3.10:</b> Block Diagram of Constant Power Laser Driver .....	<b>20</b>
<b>Figure 3.11:</b> Example Quadrant Photodiode .....	<b>20</b>
<b>Figure 3.12:</b> Quadrant Photodiode Readout Model.....	<b>21</b>
<b>Figure 3.13:</b> Example Frequency Spectrum of a Noisy Environment.....	<b>21</b>
<b>Figure 3.14:</b> Block Diagram of Lock-in Amplifier .....	<b>22</b>
<b>Figure 3.15:</b> Example PWM Waveforms .....	<b>24</b>
<b>Figure 3.16:</b> Block Diagram of Pure DC Voltage Based Motor Driver Module.....	<b>25</b>
<b>Figure 3.17:</b> Control Input Selection Model.....	<b>26</b>
<b>Figure 3.18:</b> A Screenshot from ezAFM Software.....	<b>28</b>
<b>Figure 4.1:</b> First Generation ezAFM Control Electronics and the Head Unit .....	<b>31</b>
<b>Figure 4.2:</b> First Generation ezAFM Control Electronics, showing the internal components .....	<b>32</b>
<b>Figure 4.3:</b> Latest Generation ezAFM Electronic Controller, Vibration Isolation System and ezAFM Head Unit .....	<b>32</b>
<b>Figure 4.4:</b> Topography Image of Human Red Blood Cells .....	<b>33</b>
<b>Figure 4.5:</b> Topography Image of ITO Thin Film Sample .....	<b>33</b>
<b>Figure 4.6:</b> Topography Image of Etched Pits in Mica Sample .....	<b>34</b>
<b>Figure 4.7:</b> Topography Image of Blue Ray Disc .....	<b>34</b>

<b>Figure 4.8:</b> Special Grating Sample Topography Image .....	<b>35</b>
<b>Figure 4.9:</b> iPhone 3Gs CMOS Camera Topography Image .....	<b>35</b>
<b>Figure 4.10:</b> Atomic Steps in the Gypsum Sample .....	<b>36</b>
<b>Figure 4.11:</b> Atomic Steps in the HOPG Sample .....	<b>36</b>
<b>Figure 4.12:</b> ezAFM Booth at the MRS 2012 Fall Meeting .....	<b>37</b>
<b>Figure 4.13:</b> Grains in CeO <sub>2</sub> Pellet .....	<b>37</b>
<b>Figure 4.14:</b> Proprietary Crystal Topography .....	<b>38</b>
<b>Figure 4.15:</b> ezAFM presented to the Minister of Development, President of TÜBİTAK and President of Sabancı University while it was imaging human red blood cells .....	<b>38</b>
<b>Figure 4.16:</b> Minister of Science, Industry and Technology and the industrialist Ahmet Nazif Zorlu are inspecting the ezAFM .....	<b>39</b>

# CHAPTER 1

## 1 INTRODUCTION

### 1.1 Motivation

Atomic Force Microscope (AFM) can provide 3D surface topography images of conductive, non-conductive and biological samples. Ability to see the surface structure with atomic resolution led to many novel breakthroughs in science and technology. Even though AFM is a great tool, many researchers and companies can not put their hands on any AFM systems because of the high price and the complexity of the available products. Motivation of this thesis is to design a control electronics system for an affordable, user-friendly AFM system. A low cost and high performance AFM system can also be used in the education. Not only universities, but with an affordable AFM system, high schools can also benefit from AFM also. Kids and teenagers can be exposed to the world of the Nanoscience with an AFM at very young age.

### 1.2 Outline of the Thesis

Background information about the historic and technical aspects of the Atomic Force Microscope systems will be given in Chapter 2. Later on, technical details of the ezAFM control electronics and the will be discussed in Chapter 3. Finally in Chapter 4 the images acquired with the ezAFM system will be presented.



# CHAPTER 2

## 2 BACKGROUND AND RELATED WORKS

### 2.1 Historical Background

Scanning Probe Microscopy (SPM) is a technique, which utilizes the probe surface interactions to form an image. A SPM has a precision scanner system, which scans the surface of the specimen line by line; and by doing that it records the probe surface interactions to generate an image. Scanning probe microscopy emerged after the invention of Scanning Tunneling Microscopy (STM).

STM is invented at IBM Research Lab in Zurich by Binnig & Rohrer [1] in 1981. After its invention, they were awarded with the Nobel Prize in Physics in 1986. STM uses an atomically sharp conductive tip as its probe. Under suitable conditions, STM can obtain surface topography images with atomic resolution. Atomic resolution surface image of Si(111)(7x7) sample can be seen in Figure 2.1. This image is acquired with the Ultra High Vacuum (UHV) STM system at Sabanci University “Scanning Probe Microscopy & Nanomagnetism Laboratory” located at SUNUM(Sabanci University Nanotechnology Research and Application Center).

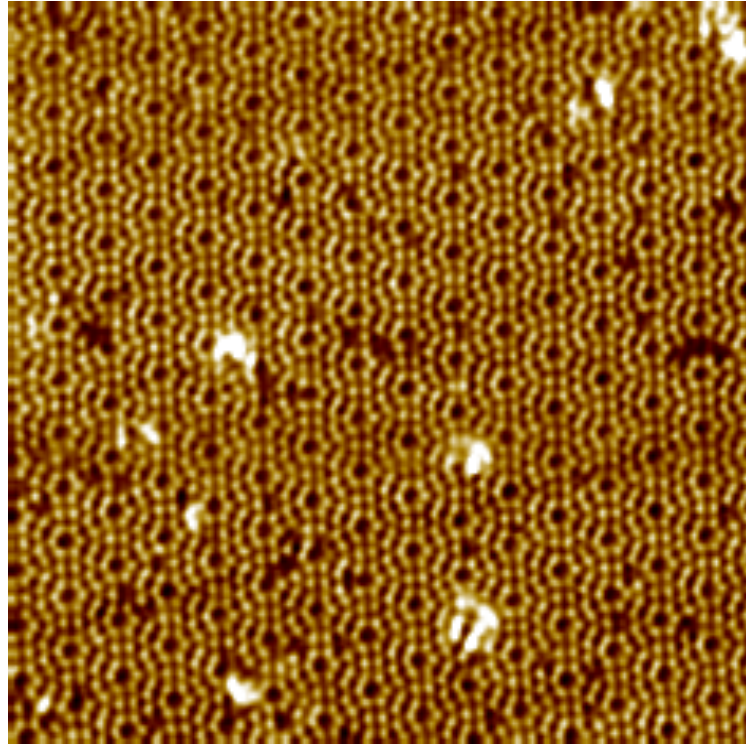


Fig 2.1: Atomic resolution surface image of Si(111)(7x7). Image Courtesy of Sabanci University - Scanning Probe Microscopy & Nanomagnetism Laboratory at SUNUM

Block diagram of the STM can be seen in Figure 2.2. A constant DC voltage is applied between the tip and sample. The tip approaches to surface with a coarse approach mechanism until a Tunneling Current (typically 0.1-1nA) is established between the sample and the surface. Tunneling current between the sample and the tip is exponentially related to the separation with a decay constant of  $\sim 2 \text{ \AA}^{-1}$ , and therefore by measuring and maintaining this tunneling current constant with a feedback control circuit, STM can scan the sample surface and create a topography image from the feedback output.

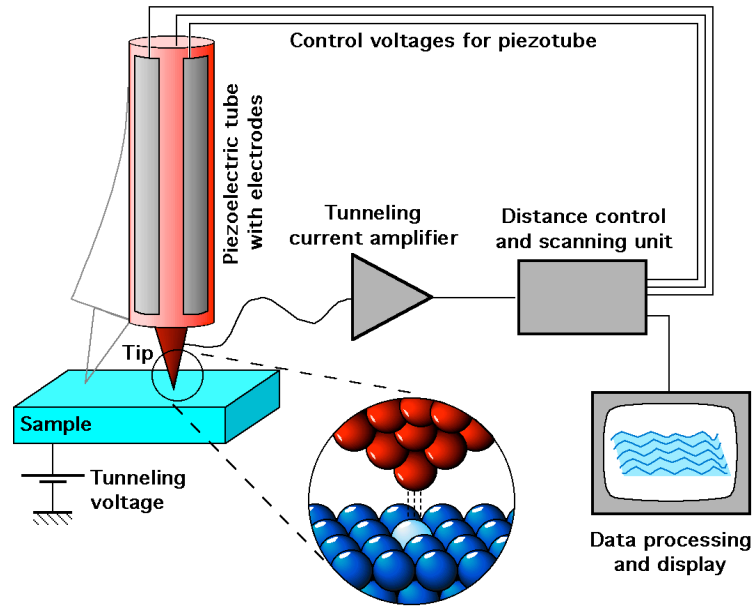


Fig 2.2: Basic Block Diagram of Scanning Tunneling Microscopy [2]

As explained above, STM needs to have a current flow between the specimen surface and the tip. Because of this, non-conductive samples cannot be investigated with the STM. This is one of the main drawbacks of the STM.

5 years after invention of the STM, AFM is invented by Binnig, Quate and Gerber in 1986 to image non-conductive samples surface topography at the atomic level. G. Binnig was also a co-inventor of the STM [3]. In the first AFM system, a tiny diamond tip is placed at the end of a cantilever produced from a thin gold foil. Subsequently, the cantilever is approached to the sample surface and the deflection of the cantilever is measured by a Scanning Tunneling Microscopy sensor, which is located at the backside of the cantilever. 2-D force map between the diamond tip and ceramic sample surface is obtained successfully with this method. In the AFM, the interaction forces between the tip and sample is utilized to measure the surface topography. A very sharp tip is placed at the end of the AFM cantilever. The other side of the cantilever is attached to a main body. The surface is scanned by touching the tip to the surface to achieve a constant normal force. A feedback circuit keeps the force between the tip and the sample constant level set by the user by moving the sample or tip with respect to each other with the Feedback Controller. The surface topography is obtained by recording the Z-position of the tip as we scan the surface line by line, while the feedback maintains a constant force. The block diagram of a typical AFM is demonstrated in Fig. 2.3

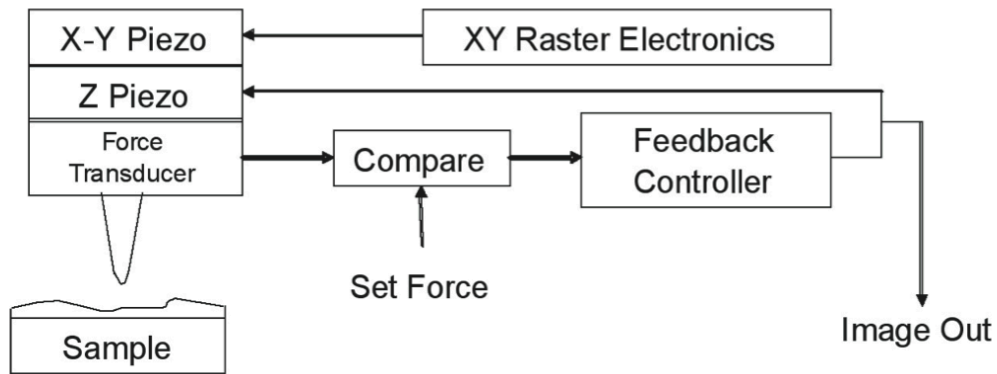


Fig 2.3: Basic Block Diagram of an Atomic Force Microcopy System [4]

## 2.2 Atomic Force Microscopy

The first Atomic Force Microscope (AFM) images are captured all in contact mode. In this mode, the tip is directly touching to the surface. The repulsive forces are active between the tip and the sample surface. Later on, Martin and his colleagues laid the foundation of the dynamic mode to measure smaller forces[5]. Cantilever, which vibrates at its resonance frequency, starts to change its oscillation amplitude when it gets a few nanometers close to the sample surface. Therefore it is possible to establish a feedback loop from the oscillation amplitude to obtain a surface topography image.

In the first AFM systems, the cantilever resonance frequency could not exceed a few kHz, because the first cantilevers were hand-made and their sizes were larger than 1mm. This factor negatively affected the scanning speed and the sensitivity. In order to overcome this problem, Albrecht and colleagues started to apply micro-fabrication techniques to produce smaller cantilevers. Si, SiO<sub>2</sub> and Si<sub>3</sub>N<sub>4</sub> AFM cantilevers are produced and with today's technology, it is possible to fabricate cantilevers with the MHz resonance frequency.

### 2.2.1 Contact Mode Atomic Force Microscopy

In the contact mode AFM, sharp tip integrated at the end of a soft cantilever, typically with a 0.01-1N/m stiffness, scans the sample surface in raster fashion by touching the surface and the surface topography is obtained by recording the Z-position of the specimen or cantilever generated by the feedback circuit, while it keeps the force constant. There are several methods to measure the deflection of the cantilever, however, because of its simplicity; Laser Beam Deflection is the most widely used

method. Since in the contact mode, tip constantly touches and interacts with the surface; this method of AFM is not suitable for very soft or fragile samples

### 2.2.2 Friction Force Microscopy

Friction force microscopy is a subset of contact mode AFM. Mate *et al.* modified the atomic force microscope to measure friction[6]. In the standard contact mode AFM, scanning direction is parallel to the cantilever. On the other hand, in friction force microscopy, surface is scanned in a direction perpendicular to the cantilever. By doing that, cantilever undergoes a torsion action because of the surface friction forces. Friction force microscopy uses this friction forces as an image forming contrast. Working principle of this microscopy can be seen in Figure 2.4.

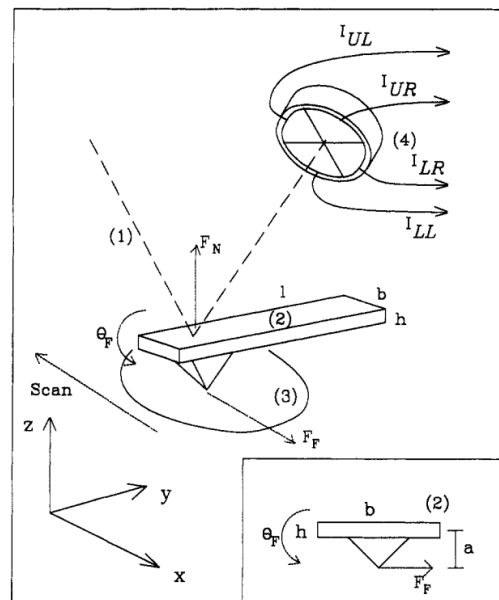


Fig 2.4: Friction Force Microscopy Principle [7]

### 2.2.3 Tapping Mode Atomic Force Microscopy

In tapping mode AFM the cantilever is vibrated at its resonance frequency. When the AFM cantilever interacts with the sample surface, oscillation amplitude starts to drop through the repulsive forces between the tip and the surface. Tapping mode AFM controls this oscillation amplitude at a constant level with a feedback loop controller to image the surface. The phase difference between the cantilever response and the excitation voltage is also recorded to obtain the phase image, which gives contrast due to different chemical and adhesion properties of the materials.

### 2.3 The Forces Measured by AFM

In order to measure the interaction between the AFM tip and the sample surface, several Scanning Probe Microscopy (SPM) techniques have been developed. The forces between the tip and surface can be divided into two basic classes: Long-range and short-range forces. Short-range forces are effective in the case that the distance between tip and the surface is shorter than 1nm and these forces are repulsive forces. If the distance between the tip and the surface is longer than 1nm, in this case the long-range forces are effective and these are impulsive forces. The chemical forces are examples of short-range forces. Electrostatic forces, magnetic forces and van der Waals forces, on the other hand, are examples of long-range forces.

The chemical forces are highly effective repulsive and attractive forces. In the region that chemical forces are active, a tiny change in the distance between tip and the surface causes drastic changes in the force. A typical force-distance curve between tip and sample is provided in Figure 2.5

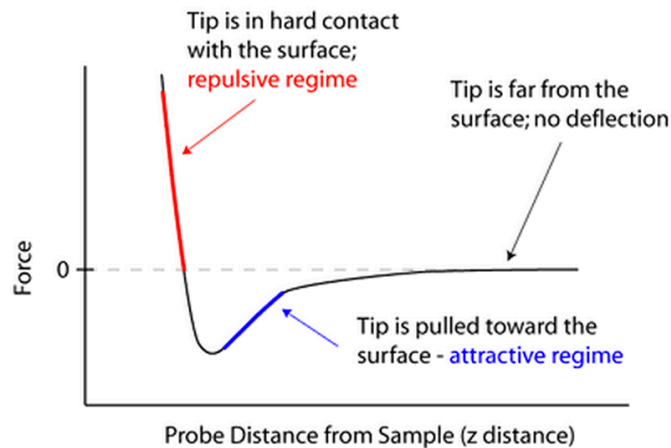


Fig 2.5: Force Distance Curve of AFM Tip [8]

Van der Waals interactions are one of the most effective attractive forces in the long-range impulsive forces category. When the cantilever gets close to the surface adequately, the surface starts to attract the cantilever and in this case, the cantilever starts to bend.

The other long-range forces are basically magnetic and electrostatic forces. If there are charges cumulated on the surface, electrostatic forces can attract or repel the AFM cantilever based on the charge density and polarity of the charge.

## **2.4 Deflection Measurement of AFM cantilever**

The detection of the cantilever deflection is one of the most critical aspects in AFM. The sensitivity of the force detection is directly proportional to the resolution of the cantilever deflection measurement mechanism. There are numerous techniques developed to detect the cantilever deflection in AFM. The first AFM developed in 1986 detected the deflection in cantilever using a tunneling sensor.

### **2.4.1 Tunneling Sensor**

While developing the first atomic force microscopy, a tunneling sensor is located at the backside of the cantilever and the deflection in the cantilever is measured utilizing the tunneling current between the tip and the cantilever. Since the application of this method is not an easy and straightforward process, scientist developed simpler techniques to detect the deflection. In addition, this method cannot sense the high-amplitude oscillations since the high-amplitude oscillations do not generate tunneling current.

### **2.4.2 Optical Beam Deflection**

The optical beam deflection method is developed by Meyer and Amer [9] and today, it is still the most-preferred deflection detection method used in AFM systems. In this method, the laser light source is focused at the back of the cantilever at a certain angle. The backside of the cantilever acts like a mirror and reflects the laser light. The reflected light is focused to position-sensitive photo detectors (PSPD). Following the deflection in the cantilever, the position of the laser light hitting on the photodiodes changes. The difference in the intensity of light between the photodiode elements is proportional to the deflection of the cantilever. By this method, the cantilever deflections in the sub-nanometer level can be measured successfully [10]. Using a quadrant photodiode, the deflection of the laser can be detected both vertical and horizontal directions. This method will be explained detail in the implementation chapter.

### **2.4.3 Piezoresistive Cantilever**

In this method cantilever itself acts as a sensor. Piezoresistive elements are micro fabricated into the special cantilevers and the leads of the resistive element on the

surface of the cantilever. AFM electronics can measure the deflection of the cantilever by measuring the changes in the resistance value, typically using a Wheatstone bridge.

## **2.5 The Scanners Used in AFM**

Low noise and accurate cantilever deflection mechanisms are not enough for AFM to properly operate alone. The cantilever has to be scanned on the surface of the sample with at least sub-nanometer resolution. There are different methods to generate such precision scanners for AFM systems.

### **2.5.1 Piezo Tube Scanners**

Piezo tube scanners are the most commonly used scanners in the AFM applications. This type of scanners generally consists of single piezoelectric tube with four separated outer electrodes. Piezo tube can be tilted along the X–Y axis by applying complementary voltages to the complementary electrodes. Movement in the Z axis can be accomplished by applying the same amount of voltage to the all four electrodes.

### **2.5.2 Piezo Stack Scanners**

Piezo stack scanners also use piezoelectric materials but the utilization of them differs from tube scanners. Stack piezo systems have two separate blocks of scanners. One of them is dedicated to the Z scanning motion and the other one is dedicated to the X Y scan motion. Stack piezo systems have much more flexibility than tube scanners since they separate Z movement axis from X-Y scan axis. Nevertheless, they still suffer from the need for high voltage source and hysteresis effects, just like the piezo tube scanners.

### **2.5.3 Voice Coil Scanners**

Voice coil AFM scanners are completely different than the piezoelectric scanners. Variable Lorentz Force can be created between permanent magnet and a coil by applying current to the coil. In the voice coil scanners Lorentz forces are used to create a precision scanner. They don't require high voltage sources to operate and they don't suffer from hysteresis problems like piezoelectric scanners. This makes the voice coil scanners easy to design and reliable options for AFM. ezAFM uses a voice coil based scanner system. Details of this scanner will be explained later.



## 2.6 Related Works

Several researchers, hobbyists and industrial companies are working on building affordable and easy to use SPM systems. One example can be seen from MIT, Department of Biological Engineering. [11] They produced an AFM for educational purposes. They utilized off the shelf Data Acquisition (DAQ) solutions and also they used MATLAB for their front-end software to create their 'teaching AFM' system. Also, several do-it-yourself approach SPMs [12][13][14] can be found in Internet. In general, they utilized a piezo disc based scanner system with analog controller, except [15] implemented DSP based digital control algorithm. Anyhow, most of these designs were one-off, hard to re-produce and usually requires high-end data acquisition systems to operate. Therefore the DIY solutions couldn't make the AFM/STM systems widely available. On the industrial side, there are a couple of products presented as educational AFM like Easyscan 2 and NAIO AFM from NanoSurf [16], AFM Workshop [17] and Nanoeducator from NTMDT [18]. Commercially available systems generally use 16bit scan DACs and ADCs, analog feedback, they do not utilize a digital lock-in amplifier as and they are still quite expensive.

# CHAPTER 3

## 3 IMPLEMENTATION

### 3.1 FPGA and Embedded Software Architecture

#### 3.1.1 FPGA Design

FPGA is the abbreviation of the Field Programmable Gate Array. Custom developed hardware can be synthesized in an FPGA by utilizing its programmable logic blocks. Custom designed hardware can include several different parallel tasks and parallel hardware blocks and FPGAs are capable of realizing such hardware. This important property of the FPGAs makes it a very attractive tool to design an FPGA based control system for AFM electronics, since AFM has many different and complicated tasks that need to be executed simultaneously.

Xilinx Spartan3A DSP series FPGA is utilized as a main controller unit for the ezAFM system. Two independent and parallel 32-bit Microblaze CPU cores are synthesized into the FPGA hardware and custom peripheral modules are written for those CPUs in VHDL language for several different requirements.

#### 3.1.2 Microblaze CPU

Soft CPU core is a microprocessor, which can be implemented in an FPGA using synthesis process. Furthermore, soft CPU cores have the flexibility of customizability at the design phase. Microblaze[19] is a 32-bit RISC Harvard architecture soft CPU designed by Xilinx. Block diagram of the Microblaze CPU can be seen in Figure 3.1.

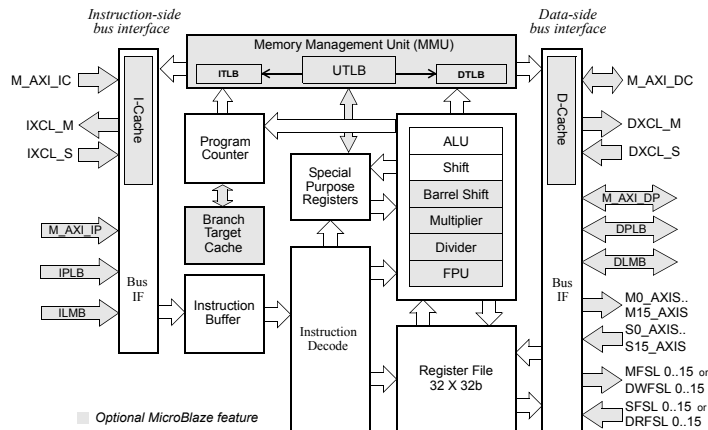


Figure 3.1: Microblaze CPU [19]

### 3.1.3 Dual CPU Design

Xilinx FPGA design environment allows users to synthesize more than one CPU core in their embedded designs. In the ezAFM system, two parallel Microblaze CPU cores are synthesized in the FPGA. Even though the FPGA allows speeds up to 90MHz, each CPU is designed to run at 50 MHz clock speed. Communication between the two CPUs is implemented using a dual port block RAM module. Block RAM is a synthesizable RAM module provided by Xilinx. Each Microblaze can access to this shared block RAM simultaneously. The values written to that shared memory place is visible for both processors.

Main Microblaze handles the communication between the PC and the hardware and performs the tasks assigned by the PC. Details of the controller - PC communication and task assignment procedure will be discussed later. While the main Microblaze is occupied with the time consuming and blocking tasks, slave Microblaze is in charge of data acquisition and the AFM feedback control tasks. Since those two CPUs are physically independent from each other, control loop and data acquisition task continues with a consistent timing without any interventions.

### 3.1.4 Custom Peripheral Core Implementation

Several custom peripheral cores were implemented to reduce the computation load of the Microblaze CPUs synthesized into the FPGA. Custom cores of the ezAFM are

written using VHDL. A register-based interface is constructed between Microblaze CPU and the custom cores. Each custom core has limited number of 32-bit data registers, which can be directly accessible from the Microblaze over *Peripheral Local Bus* (PLB) interface. For instance, ADC driver core generates necessary clock and data signals by custom hardware written in VHDL and then records the latest ADC values into the data-registers. Later on, Microblaze can read the latest ADC results with minimal effort, only by accessing necessary peripheral registers.

### **3.2 Embedded Software Design**

Xilinx offers Eclipse based software design environment for the Microblaze CPUs. C programming language is used for developing firmware for the Microblaze CPUs.

### **3.3 Data Acquisition**

AFM systems have to monitor several analog signals simultaneously while generating necessary control and scanning signals. To accomplish this in digital domain, data acquisition systems are required. Analog to digital converters and the digital to analog converters are the fundamental building blocks of the digital data acquisition systems.

The slave Microblaze handles data acquisition task in the ezAFM. This task involves reading analog voltage values from ADC driver core and storing them into the shared RAM, reading phase and amplitude information from digital lock-in amplifier core and storing them into the shared RAM and sending analog voltage values to the DAC driver core by looking at the values at the shared RAM. At anytime main Microblaze core can read or write the necessary shared RAM location to monitor, record or change the analog voltage values.

### **3.4 Voice Coil Scanner Design**

As it explained in the introduction, a precision scanner is an important building block of the AFM systems. Voice coil based scanner system is used to design the precision scanner for the ezAFM system. Four different voice coils are used to implement the

scanner, which is capable of making 3-axis precision movements with sub-nm precision.

Voice coils basically consist of one permanent magnet and a coil, which acts as an electromagnet. Placement of the two magnets can be seen in Figure 3.2.

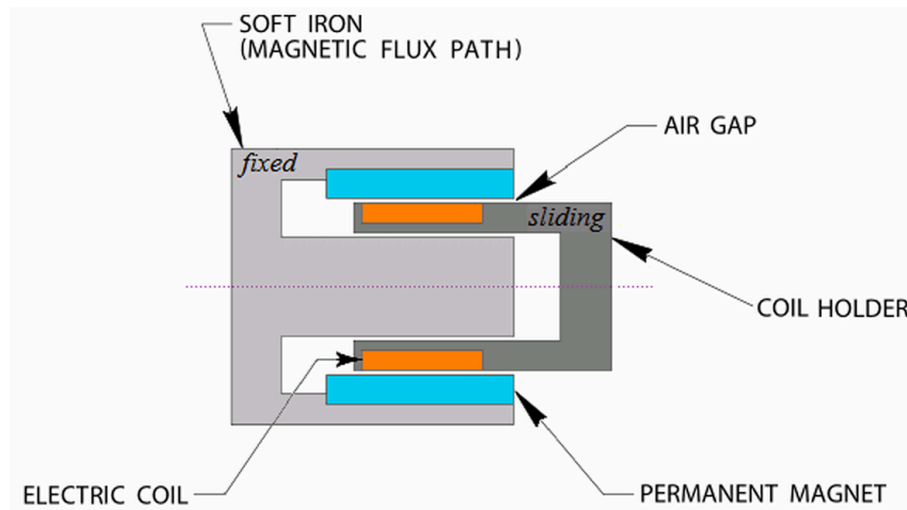


Figure 3.2: Operating Principle of Voice Coil Actuator

When current starts to pass through the voice coil, a force between the voice coil and electromagnet starts to emerge. According to the Lorentz principle [20] this force can be written as follows.

$$F = k * B * L * N * i$$

$k$  is a constant  $L$  is the length of the coil,  $N$  is the number of windings of the coil,  $i$  is the current passing through the coil and  $B$  is the magnetic flux density in the gap. Magnetic flux density generated by the permanent magnet and other parameters of this formula is fixed. Therefore the direction and the amount of linear displacement of the voice coil depend on just the current passing from the coil and the stiffness of the mechanism on which the coil is attached.

### 3.4.1 Driver Mechanism

The block diagram of voice coil driver mechanism can be seen in Figure 3.3. X, Y and Z coordinates of the scanner are calculated by the Microblaze CPU then another logic block calculates individual voltage values which must be applied to each coil in order to move the scanner to that desired position.

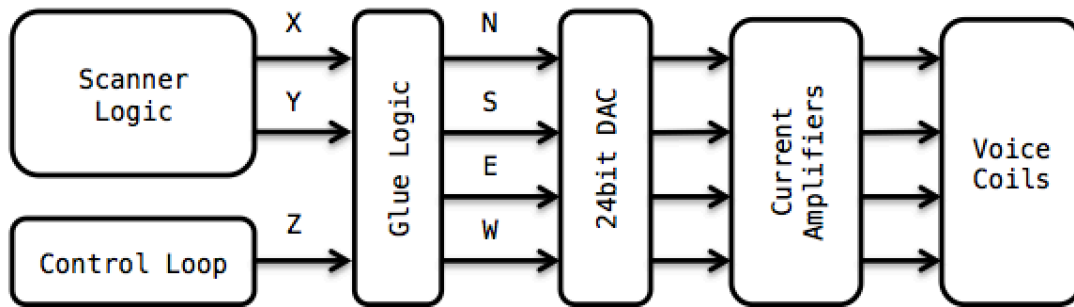


Figure 3.3: Block Diagram of Voice Coil Scanner Electronics

Scan voltages are generated by 24bit DACs. Outputs of these DACs then go into the current amplifiers, which generate necessary current values with respect to the DAC voltage outputs.

### 3.4.2 Advantages Over Piezoelectric Scanners

Voice coil based scanners don't need to use high voltage sources; therefore the scanner and the driver electronics can become more compact and simpler to design. Piezoelectric scanners need voltages in the order of couple hundred volts to operate. Moreover, piezoelectric scanners suffer from hysteresis and creep effects, which creates the necessity to use several software correction algorithms [21] [22] [23] [24]. On the contrary the voice coil scanners have linear current – displacement characteristics and therefore they are much easier to design and they are more reliable.

### 3.5 Cantilever Excitation

Cantilever excitation mechanism is a must for the tapping mode AFM. In the tapping mode AFM, as it also explained in the introduction, cantilever is excited with its resonance frequency value. Such an excitation mechanism is implemented by using a small dither piezo. Dither piezo is a small piezoelectric material, which doesn't require

any high voltage or high current source and can be driven directly with an op-amp. Basic block diagram of the implemented system can be seen in Figure 3.4.

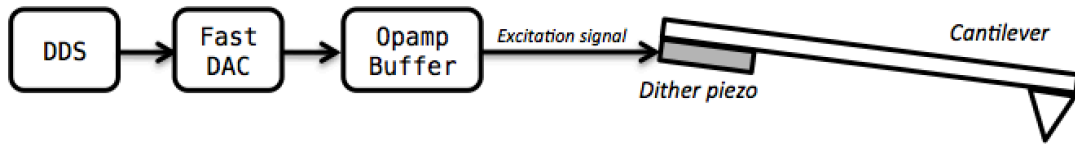


Figure 3.4: Block Diagram of Cantilever Excitation System

### 3.5.1 Excitation Frequency Tuning

Cantilever can be thought as a simple LC tank circuit in electronics, which means that the cantilevers have very sharp frequency response curves to the applied forces. Therefore a specific resonance frequency has to be found for each cantilever in order to get the maximum oscillation.

In order to tune this resonance frequency, basic frequency spectrum analysis algorithm has been implemented at the control electronics and corresponding GUI element has added to the PC side software. User enters start and finish frequency values and the control electronics sweeps the excitation frequency within the specified range. While the system sweeps the frequency output, it also records amplitude and phase of the cantilever deflection at each step. In Figure 3.5, an example screenshot from a tuning session can be seen. The frequency, which gives the highest oscillation amplitude, is the resonance frequency.

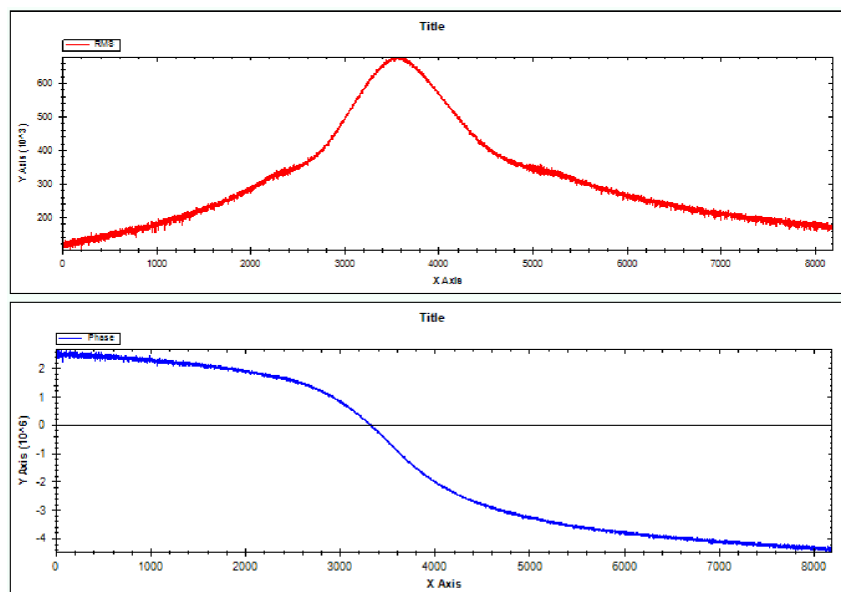


Figure 3.5: Phase and Frequency Response of a Cantilever

Resonance frequency of the cantilevers is generally between 100 and 300 kHz range. Direct Digital Synthesizer implemented in FPGA hardware in order to generate digital sinusoidal frequency value samples at that frequency range.

### 3.5.2 Direct Digital Synthesizer (DDS)

Direct Digital Synthesizer can synthesize sinusoidal, or any kind of periodic signal, at different frequencies by using a limited quantity lookup table. When setting the output of the DDS to a different frequency, there is no need to change the lookup table values. This flexibility is one of the most important advantages of the DDS. Block diagram of a simple DDS can be seen in Figure 3.6.

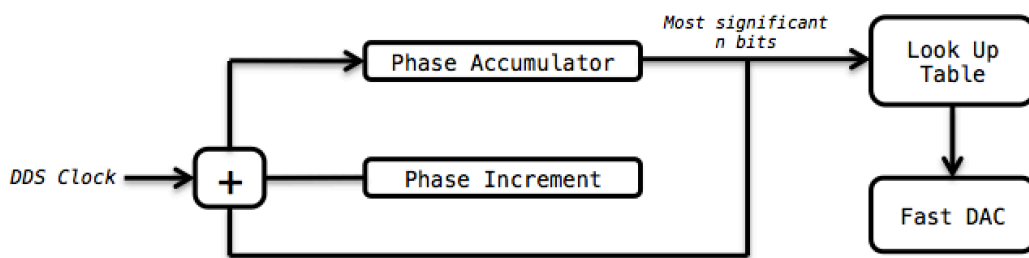


Figure 3.6: Block Diagram of a Simple DDS Module

Frequency adjustments are done with changing the phase increment value. In each clock cycle, phase accumulator register is incremented with that specified increment number. Afterwards, that incremented phase accumulator value is used to select a value from a look up table (LUT) and then resulting value is being written to the DAC. At the best scenario, all phase register values is assigned to a specific LUT value but in memory constrained situations, selected number of higher order bits of the phase accumulator can be used to index the lookup table in order to shrink the size of LUT.

Output frequency of the DDS can be calculated as follows:  $N$  indicates the bit size of the phase accumulator register.

$$f_{output} = \frac{f_{clock} * phase\_increment}{2^N}$$

The frequency resolution of the DDS module described as follows:



$$f_{resolution} = \frac{f_{clock}}{2^N}$$

Phase accumulator in our implementation has 32bit width and the DDS master clock is 12.5 MHz. In order to create a decent sinusoidal signal at the 300kHz range, fast sampling DAC with 16bit resolution is used. The frequency resolution of our DDS is 2.9 mHz.

### 3.6 Cantilever Deflection Measurement System

A low noise measurement system for cantilever deflection is necessary for the AFM. As explained in the introduction, there are several different methods for cantilever deflection measurement. In this thesis, laser beam deflection system [25] is implemented as shown in Figure 3.7.

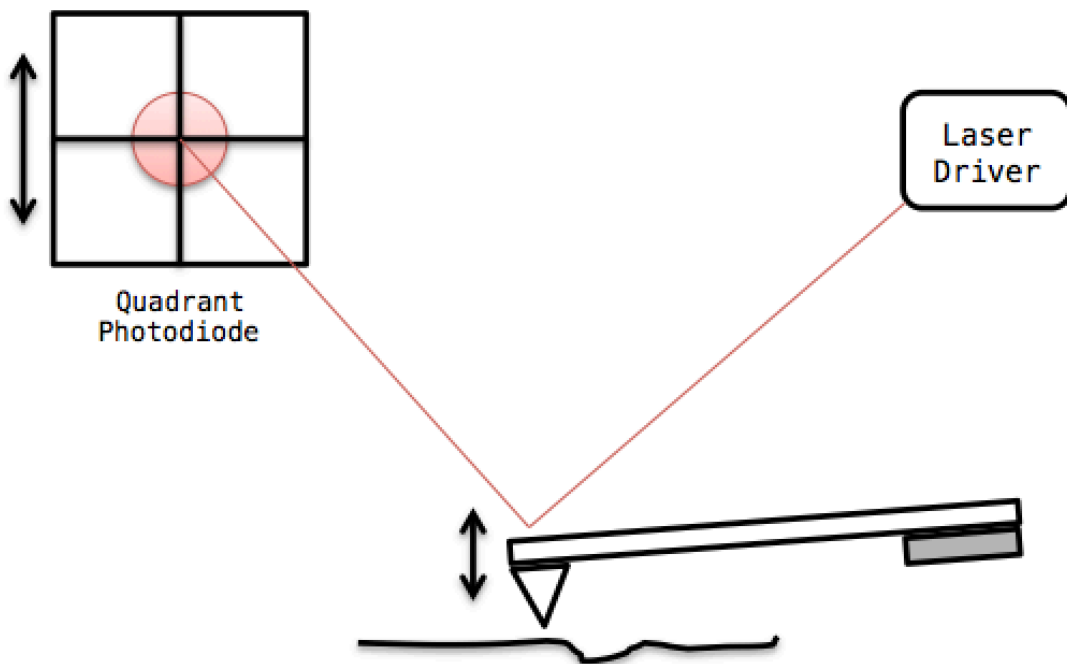


Figure 3.7: Laser Beam Deflection Measurement

#### 3.6.1 Constant Power Laser Driver

Constant power laser driver is a fundamental requirement for an Atomic Force Microscope. All of the control mechanisms are directly affected from the laser power. For example, if laser output power starts to drop while scanning, control loop cannot distinguish whether that the surface interaction is changed or it is a just temperature

caused drift. Therefore, control loop tries to arrange the Z-axis voltage accordingly to compensate the laser power drop for no reason and the resulting image will be badly affected.

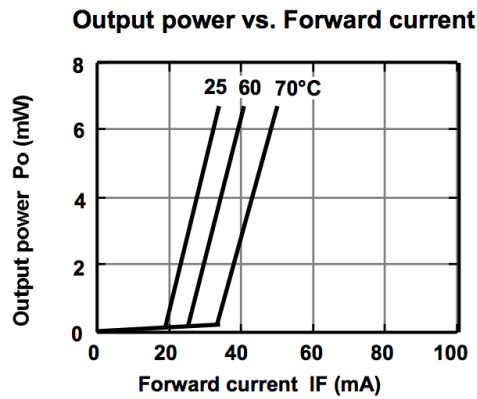


Figure 3.8: Output Power – Forward Current Graph of a Laser Diode

In Figure 3.8 forward current – output power graph of a typical laser diode can be seen. As it can be seen from the graph, even though applied current is kept stable, at each different temperature, diode’s output power and whole characteristics are changing. Therefore, designing a constant current source to drive the laser diode is not a robust solution.

Since it is a known problem among the laser diode users, manufacturers have been integrating a photodiode inside the laser diodes packages to give users capability to monitor laser diodes output power. Example monitor photodiode current vs. laser-diode output power can be seen in Figure 3.9.

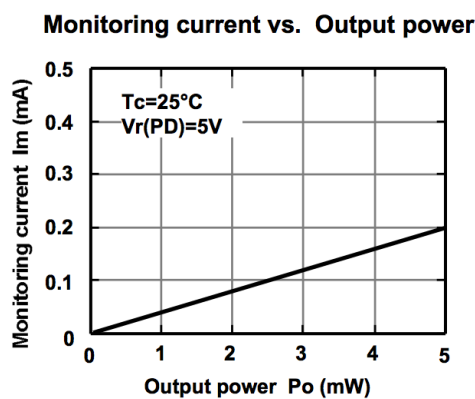


Figure 3.9: Monitor Current – Output Power Graph of a Laser Diode

As it can be seen in the Figure 3.9 output power vs. photodiode current is changing linearly. Therefore it is best to design a circuit, which monitors the photodiode current and tries to maintain it constant. Block diagram of such a circuit can be seen at Figure 3.10.

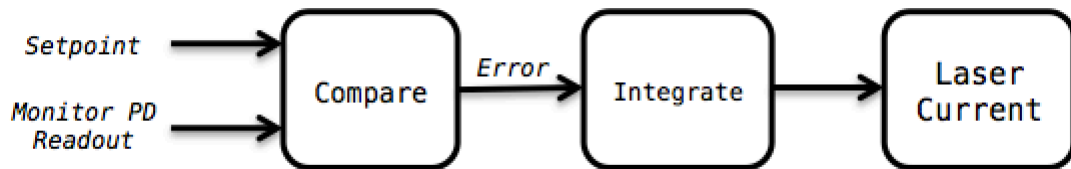


Figure 3.10: Block Diagram of Constant Power Laser Driver

Opamp based analog implementation of this system is realized in the ezAFM.

### 3.6.2 Quadrant Photodiode Readout

Quadrant photodiode is a special purpose photodiode, which consists of four equally separated quadrant photodiodes in a single case. A typical quadrant photodiode can be seen in Figure 3.11.

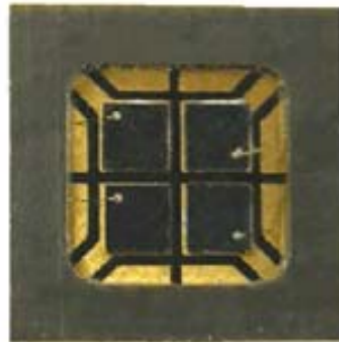


Figure 3.11: Example Quadrant Photodiode

During the construction phase of the AFM, orientation of the laser and the photodiode is arranged accordingly such that, the reflected laser beam from the cantilever hit the center spot of the quadrant photodiode. In Figure 3.12 desired situation can be seen. In that desired situation, each four of the quadrants gives the same readout value which indicates that without any surface sample interaction, or without any cantilever deflection exists, all four of the quadrants gives the same readout value. Lateral and

normal deflection of the cantilever can be calculated. Difference between the upper and lower quadrants gives the normal deflection information and the difference between left and right quadrants gives the lateral deflection information. Illustration of this model can also be seen in Figure 3.12.

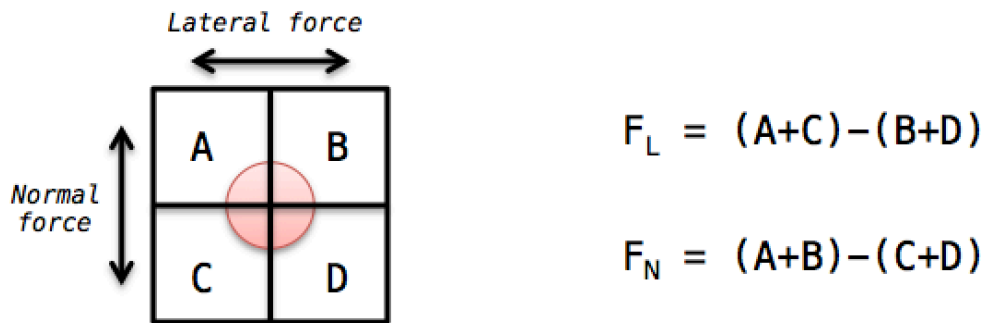


Figure 3.12: Quadrant Photodiode Readout Model

In the ezAFM system, calculations of lateral force and normal force values are implemented in analog domain using opamps.

### 3.6.3 Digital Lock-in Amplifier (LIA) Implementation

Tapping mode AFM takes the oscillation amplitude of cantilever as a control input; therefore it is required to calculate the amplitude of oscillation voltage. Oscillation frequency of the cantilever deflection is in the range of approximately 100-300 kHz. In order to calculate the amplitude of such signals, lock-in amplifier in FPGA hardware is implemented.

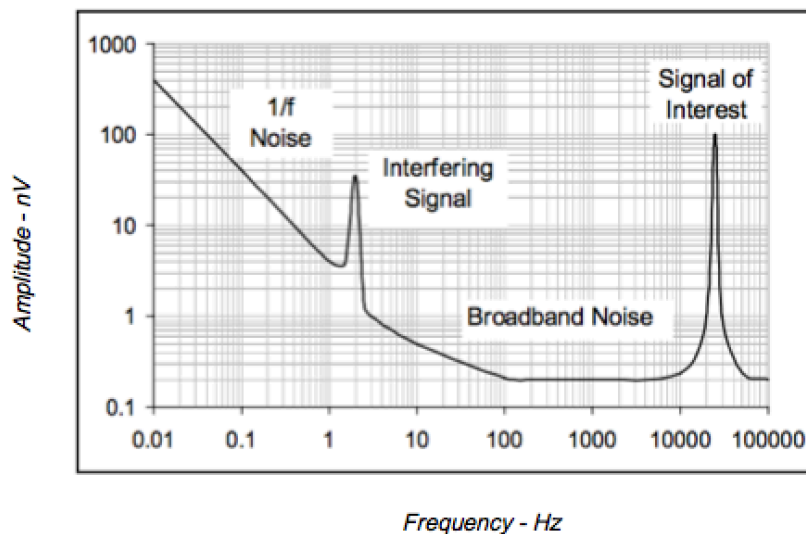


Figure 3.13: Example Frequency Spectrum of a Noisy Environment [26]

The main purpose of a lock-in amplifier is measuring a small signal's amplitude and phase information in a noisy environment. [27] By actively selecting only the specific frequency, the noise distributed across the whole frequency spectrum is also eliminated. Several noise sources from the frequency spectrum can be seen in the Figure 3.13

### 3.6.3.1 Mathematical Background of Lock-in Amplifier

Basic block diagram of the lock-in amplifier can be seen in Figure 3.14

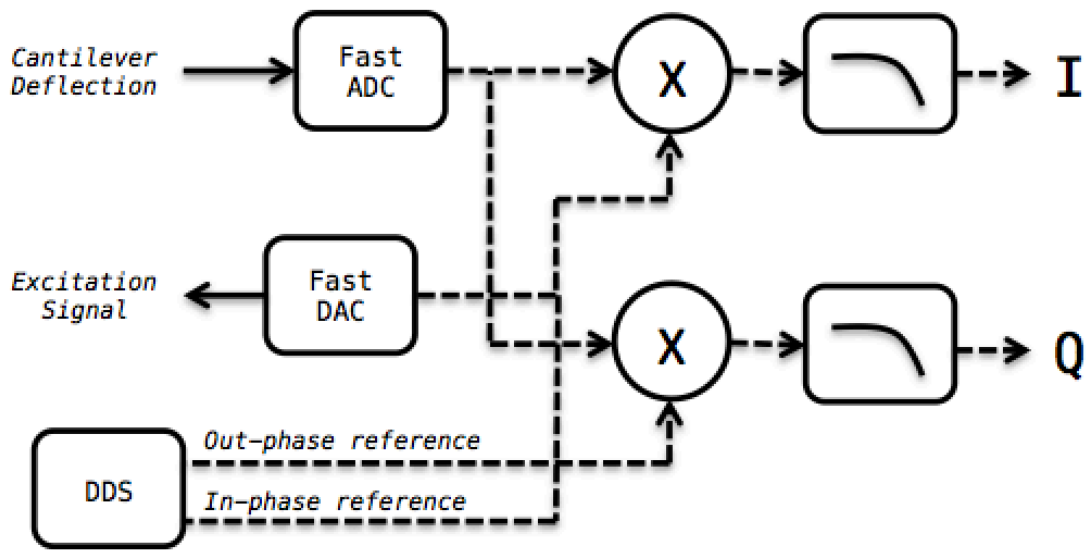


Figure 3.14: Block Diagram of Lock-in Amplifier

Local oscillator of the lock-in amplifier generates two sinusoidal signals with same frequency  $f$  but  $90^\circ$  phase shifted from each other. Those two signals are named as  $ref_{inPhase}$  and  $ref_{outPhase}$ .

$$ref_{inPhase} = A * \sin(2\pi f)$$

$$ref_{outPhase} = A * \sin\left(2\pi f + \frac{\pi}{2}\right)$$

$ref_{inPhase}$  signal is converted into analog domain using a fast 16Bit DAC and is applied to the dither piezo which oscillates the cantilever. The measured cantilever deflection signal is the phase shifted and amplitude changed version of the  $ref_{inPhase}$  signal.

$$signal_{meas} = B * \sin(2\pi f + \theta)$$

Measured input signal is converted into digital domain using a fast 16Bit ADC and then multiplied by the in phase oscillator signal and out of phase oscillator signal separately in the digital domain.

$$\begin{aligned} \mathit{ref}_{inPhase} * \mathit{signal}_{meas} &= A * B * \mathit{Sin}(2\pi f) * \mathit{Sin}(2\pi f + \theta) \\ \mathit{ref}_{outPhase} * \mathit{signal}_{meas} &= A * B * (\mathit{Sin}\left(2\pi f + \frac{\pi}{2}\right) * \mathit{Sin}(2\pi f + \theta)) \end{aligned}$$

When the necessary trigonometric conversions have applied, following result can be obtained.

$$\begin{aligned} \mathit{ref}_{inPhase} * \mathit{signal}_{meas} &= A * B * (\mathit{Sin}(4\pi f) + \mathit{Sin}(\theta)) \\ \mathit{ref}_{outPhase} * \mathit{signal}_{meas} &= A * B * (\mathit{Sin}\left(4\pi f + \frac{\pi}{2}\right) + \mathit{Sin}\left(\theta + \frac{\pi}{2}\right)) \end{aligned}$$

Output of this multiplier is then connected to a low pass filter, which filters the signal at the high frequencies. Results of these two low pass filters are called  $I$  and  $Q$  (in phase and quadrature).

$$\begin{aligned} I &= A * B * \mathit{Sin}(\theta) \\ Q &= A * B * \mathit{Cos}(\theta) \end{aligned}$$

After  $I$  and  $Q$  signals are calculated, the phase difference between applied reference signal and the measured signal  $\theta$  can be calculated as follows.

$$\begin{aligned} \frac{I}{Q} &= \frac{\mathit{sin}(\theta)}{\mathit{cos}(\theta)} = \mathit{tan}(\theta) \\ \theta &= \mathit{atan}\left(\frac{I}{Q}\right) \end{aligned}$$

Moreover, the amplitude of the input signal also can be calculated as follows.

$$\begin{aligned} I^2 + Q^2 &= (A * B)^2 * (\mathit{sin}^2(\theta) + \mathit{cos}^2(\theta)) \\ \mathit{sin}^2(\theta) + \mathit{cos}^2(\theta) &= 1 \\ I^2 + Q^2 &= (A * B)^2 \\ \sqrt{I^2 + Q^2} &= A * B \end{aligned}$$

$$B = \frac{\sqrt{I^2 + Q^2}}{A}$$

### 3.6.3.2 Digital Implementation

The ezAFM lock-in amplifier is implemented in FPGA hardware. A 100 MSPS 16Bit fast ADC is used to sample the deflection signal. Second order infinite impulse response (IIR) filters are used for the low pass filters. SQRT and ATAN algorithms are implemented in FPGA hardware using Xilinx's Coregen [28] tools. Implemented lock-in amplifier hardware is interfaced to the Microblaze CPU via PLB bus as a custom peripheral.

### 3.7 Coarse Approach Mechanism

In AFM measurement system all the samples which user wants to image do not have the same height/thickness. Furthermore the scanners have limited scan ranges with respect to the thickness changes among the samples. Therefore a coarse approach mechanism to bring the sample holder within the scanner's range is required. Single high reduction ratio DC gear-motor is used to create the coarse approach mechanism. Linearity of the movement is achieved thanks to the linear bearings utilized at the AFM head.

It is a very standard conception to use PWM signal to control the speed of a motor. PWM stands for the Pulse Width Modulation. An example PWM waveform can be seen in Figure 3.15. When PWM signal is applied to a motor, its effective speed can be controlled by the duty cycle of the PWM signal.

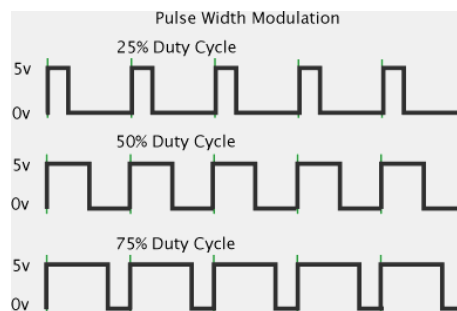


Figure 3.15: Example PWM Waveforms

Discontinues of the PWM signal creates a problem. Since the proposed AFM head is stabilized by the tight springs, oscillations occur due to sharp edges and high frequency components of PWM signals even after small movements.

After identifying this problem, a direct DC drive electronics is implemented to control the motor. By applying pure DC voltage to drive the motor, spikes caused by the PWM signal is prevented. Block diagram of the implemented system can be seen in Figure 3.16. Motor direction is also controllable by generating effective positive or negative current across the DC motor.

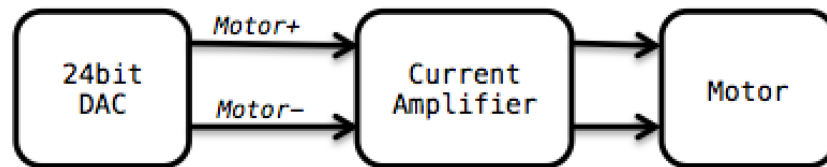


Figure 3.16: Block Diagram of Pure DC Voltage Based Motor Driver Module

### 3.8 Feedback Control System Design

A reliable feedback control system is required for all of the operating modes of the AFM. In tapping or dynamic mode AFM, the cantilever oscillation amplitude is kept constant by the feedback circuit by moving the specimen or cantilever in Z direction as we scan the tip across the surface. In contact mode AFM the force itself is kept constant by the feedback circuit.

Initially AFM controllers were implemented in fully analog domain. This implementation has its advantages like to the much higher control bandwidths and quicker response rates but analog controllers are hard to tune. Most of the analog controllers use digital potentiometers or programmable gain amplifiers to adjust the gain but the amount of the control is limited. In this thesis fully digital control system is implemented for ezAFM. Research AFMs like [29],[30],[31] and most commercial AFMs from Bruker, Asylum also implemented fully digital feedback controllers in their AFM designs.

Measurement input of the system is cantilever deflection voltage, which is calculated by the analog quadrant photodiode readout circuit. According to the working mode of the AFM, representation of this voltage changes. For instance, in the tapping mode we are interested in the AC content of the deflection voltage, whereas in the contact mode DC content of the deflection signal has to be used. Therefore, quadrant photodiode readout



voltage is buffered twice and sampled simultaneously with two different ADC systems. AC coupled version of the deflection voltage is sampled with the fast sampling 16Bit ADC and it is used as the input to digital lock in amplifier. The DC coupled version is sampled with standard 24bit ADC after low pass filtering. Block diagram of this model can be seen in Figure 3.17.

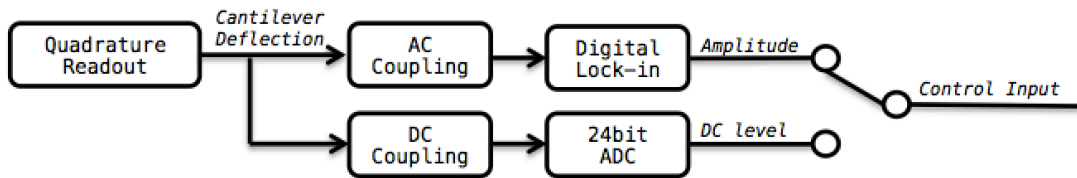


Figure 3.17: Control Input Selection Model

As it explained in the previous sections, control system tries to keep the measurement input at a constant set point by actuating the Z-axis of the precision voice coil scanner. Therefore, the output of the control system defines the Z-axis location of the scanner.

### 3.8.1 Digital Feedback Algorithm

A PID control algorithm is implemented for the ezAFM system. PID is the abbreviation of Proportional Integral Derivative. Error is the difference between measured input value and the desired set point value. PID control algorithm decides on its output value not only by looking at the current error value, but also looking its rate of change and integral over the time. Therefore it can create a more robust control solution.

When only the proportional control is used, constant offsets between the set point and measured signals can occur. Main reason for this is that most actuators have a required minimal actuation force and below that force actuators nearly doesn't response to given inputs at all. This problem can be cured by increasing the  $P$  coefficient, but the system becomes more instable and oscillations emerge as a side effect.

Integral coefficient of the PID algorithm tries to reduce this constant offset problem caused by the proportional controllers. Integral part of the algorithm accumulates the errors and multiplied version of this accumulated error ads up to the control output. Small error values, which normally cannot generate any actuation on the system with

only proportional control, accumulates and creates enough system output and those small error values can be eliminated with a smaller proportional gain settings.

Last part of the PID algorithm is the derivative part. Derivative part of the PID control algorithm basically acts as a damping mechanism for the system output. In each sampling interval, derivative of error curve is calculated. Later on that calculated derivative is multiplied by a constant and subtracted from the addition of proportional and integral contributions and applied to the actuator as a system output. Derivative of the error in the control loop represents the amount of speed that system reacts to the given input. Without derivative coefficient system first overshoots and then settles, but derivative part enables the system to reach to the set point without, or less, overshoots by slowing the effects of the proportional and integral contributions of error.

### **3.8.2 Implementation Details**

Control algorithm is realized on the Microblaze CPU dedicated to data acquisition and control system implementation, which is synthesized on the FPGA fabric. Real time PID control algorithm is written in C language and has 60 kHz update rate. Parameters of the algorithm are completely adjustable from the computer interface.

### **3.9 PC Software Design**

Computer interface of the ezAFM is built upon existing SPM control application written by NanoMagnetics Instruments using C#. Hardware interface parts of the existing software were deleted and new hardware interaction layer was written for the new hardware. Also several algorithmic changes were made to benefit from the new Digital Control Electronics. Example screenshot from ezAFM software can be seen in Figure 3.18.

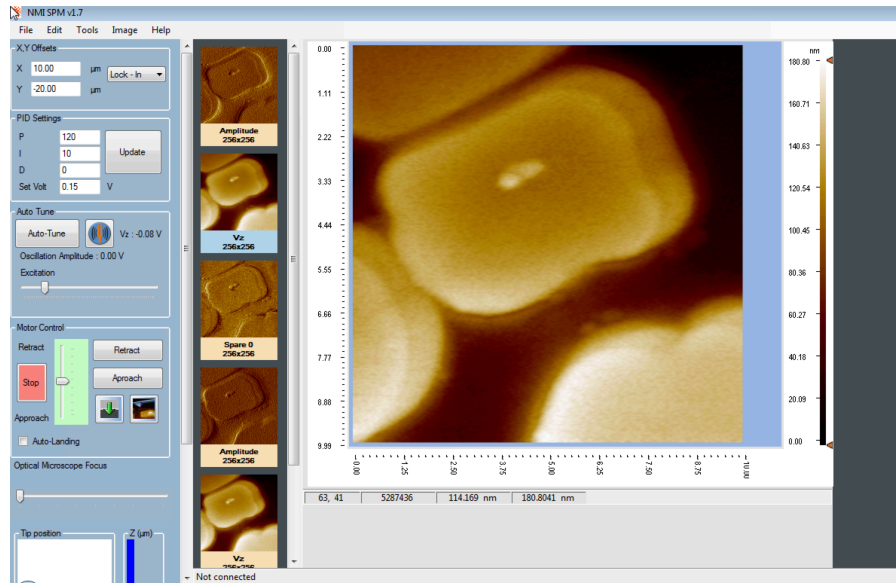


Figure 3.18: A Screenshot from ezAFM Software

### 3.10 Communication Hardware Details

PC and the ezAFM control electronics are communicating over 480 Mbit/s USB 2.0 High Speed interface. In the hardware side, Cypress FX2 microcontroller is utilized for USB communication and this microcontroller is interfaced to the main Microblaze CPU through a FIFO based custom peripheral module. Custom peripheral module gives basic push/pop based FIFO access to the USB endpoints for communication.

### 3.11 Communication Architecture

As it explained in the previous section, two parallel Microblaze CPUs are synthesized in the FPGA fabric. Without PC intervention the master Microblaze waits in an idle state and does nothing until a command has been sent by the PC. On the other hand slave Microblaze never stops its data acquisition task and control task.

The PC side always controls the communication between the computer and the control electronics. PC always sends a request to the ezAFM Control Electronics and then the main Microblaze exits its idle state, performing the required tasks in communication with the slave Microblaze and then sends the requested data back to the PC and returns into the idle mode.

Two main types of communication between occur between the PC and the ezAFM Control Electronics. First type is the periodic updates. PC software request fixed

amount of data with a predefined interval to update several GUI elements. Status value of the electronic hardware, several analog voltage values and lock-in amplifier readouts are included in this fixed amount of data. PC stops requesting this periodic update when it assigns a task to the electronic controller.

Second type of communication is the task assignment requests. This type also includes two different subcategories. Tasks can be instant or blocking. Instant tasks don't take too much time on the ezAFM electronics controller. Therefore, the PC doesn't explicitly check whether it finished that task is not. Updating motor voltage, changing excitation signal amplitude or updating PID coefficients can be given as examples for instant tasks. Blocking type of tasks is much different than the instant tasks

### **3.12 Task Assignment Approach**

Blocking assignment type communication basically assigns a specific task to the ezAFM and blocks the GUI interaction until the control electronics responses. As it also explained above, during that blocking time interval, periodic update requests are also stopped to prevent any intervention to the assigned task. Assigning tasks to the ezAFM brings real-time performance and speed advantage. Generation of the scanning signals in ezAFM is one of the example to show this.

Normally AFM systems uses control electronics as non-intelligent data acquisition extensions and therefore they manually generate control signals and store the image data values at discrete pixel steps from the PC side. PC side applications cannot generate fixed interval signal. There always will be unexpected latencies caused by the operating system and the background application. Moreover, in order to make a full scan with a 24 bit resolution by this approach, more than 16 billion requests have to be sent for each line.

ezAFM uses task assignment approach to address these issues. User sets the scanning area size, scanning speed and the pixel resolution information from the GUI. According to the user input, PC software calculates the boundaries of the scan signal and sends to the control electronics. Hardware controller generates the scan signals without any interventions in strict timing and records the necessary imaging elements like Z axis voltage, phase voltage etc. in the DDR memory connected to the FPGA. After the line

scan ends, master Microblaze pushes one byte data into USB endpoints to signal the PC. After PC software gets the signal, it sends another request to fetch the necessary scanning line scan data stored on the DDR memory from the hardware.

# CHAPTER 4

## 4 RESULTS AND CONCLUSION

### 4.1 Prototypes

Two consecutive generations of ezAFM systems has been built. First one was completed in March 2012. That version was using a 16Bit data acquisition system. Moreover, the cantilever deflection amplitude was being measured by off the shelf RMS to DC converter IC. Images of the first generation electronic controller can be seen in Figure 4.1 and Figure 4.2.



Figure 4.1: First Generation ezAFM Control Electronics and the Head Unit

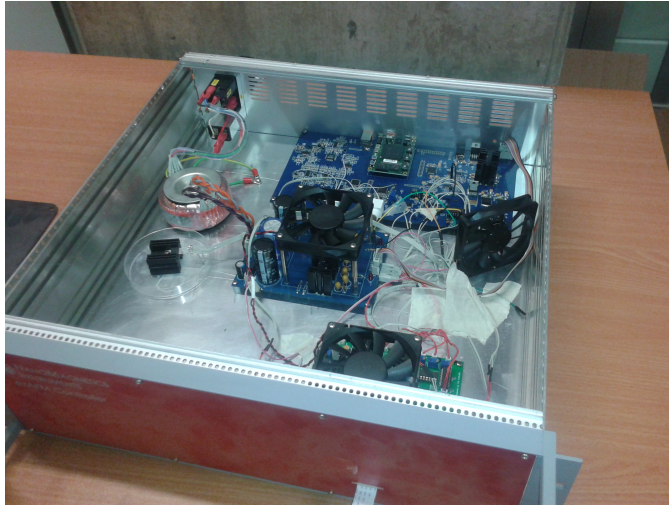


Figure 4.2: First Generation ezAFM Control Electronics, showing the internal components

As it can be seen from the images, first unit built was a ‘proof of concept’; therefore size and complexity wasn’t issue. Nevertheless it had a fully digital feedback controller system and it was communicating with the PC over High Speed USB2.0 data link.

Later, the second-generation ezAFM was built. This latest version is using 24-bit data acquisition system and also includes a digital lock-in amplifier. Furthermore the size of the electronics case has been reduced dramatically. Figure 4.3 shows the finished version of the second-generation ezAFM.



Figure 4.3: Latest Generation ezAFM Electronic Controller, Vibration Isolation System and ezAFM Head Unit

## 4.2 Images

Selected images acquired by the ezAFM in tapping mode using Tap150 cantilevers from Budgetsensors can be seen in the following section.

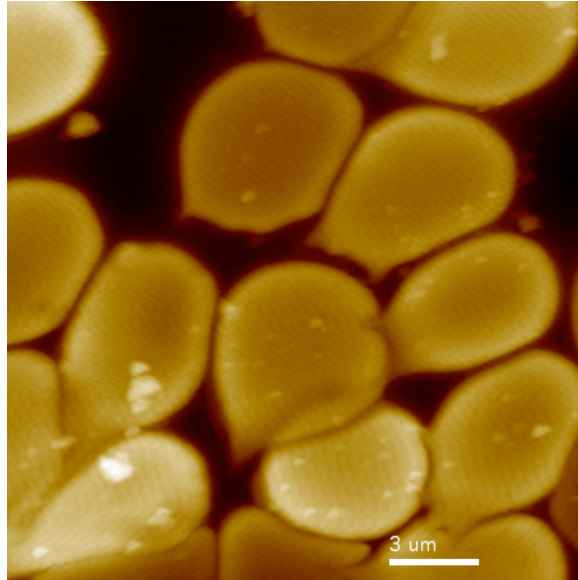


Figure 4.4: Topography Image of Human Red Blood Cells

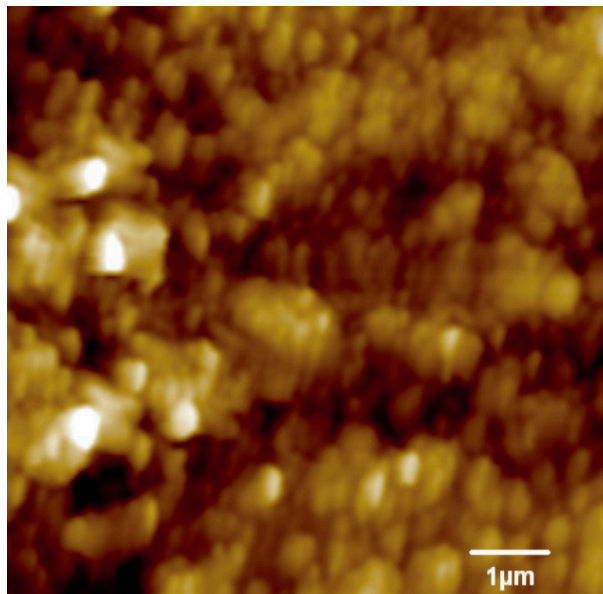


Figure 4.5: Topography Image of ITO Thin Film Sample



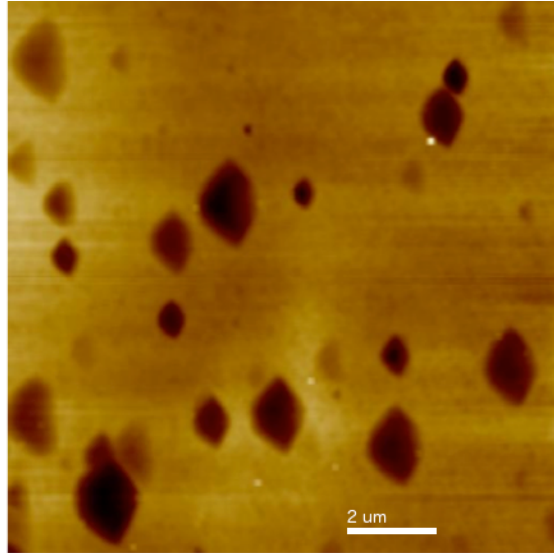


Figure 4.6: Topography Image of Etched Pits in Mica Sample

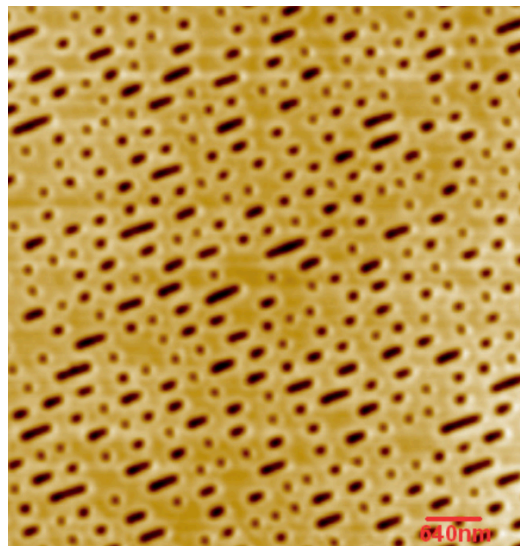


Figure 4.7: Topography Image of Blue Ray Disc

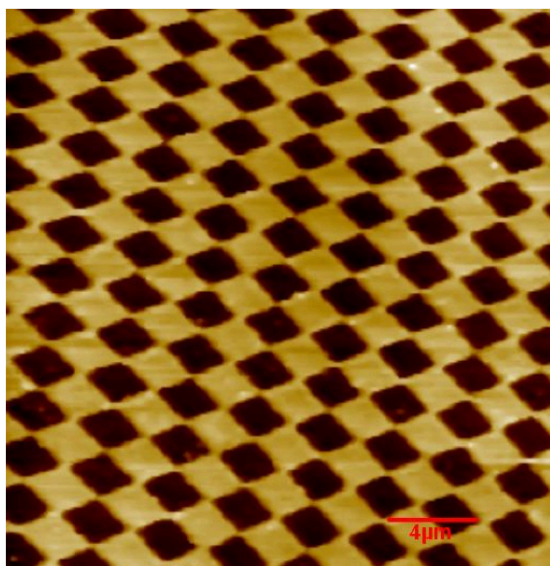


Figure 4.8: Special Grating Sample Topography Image

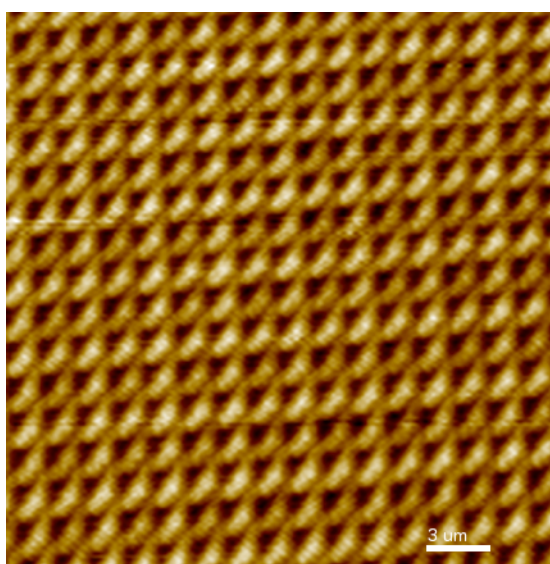


Figure 4.9: iPhone 3Gs CMOS Camera Topography Image

Atomic steps in the Gypsum and HOPG also can be imaged by the ezAFM.

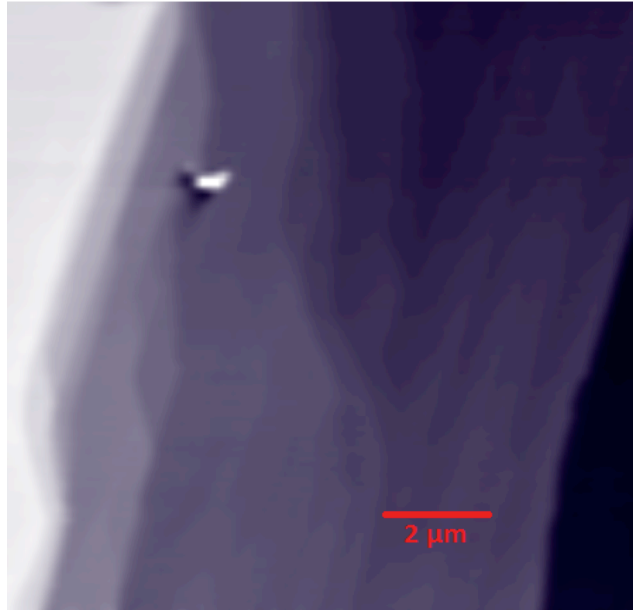


Figure 4.10: Atomic Steps in the Gypsum Sample

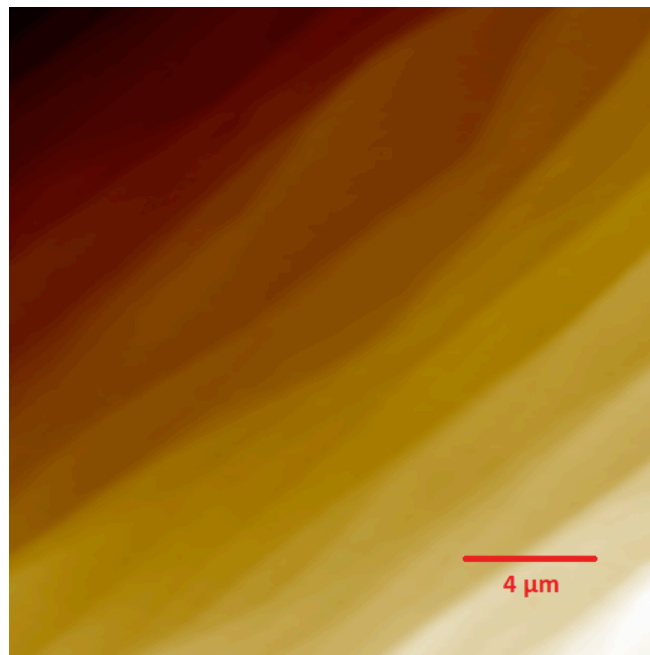


Figure 4.11: Atomic Steps in the HOPG Sample

### 4.3 Publicity

Initial design results of the ezAFM are presented at the APS 2012 March Meeting [32] Furthermore, two operational ezAFM systems are presented in the MRS 2012 Fall Meeting. Images from this event can be seen in Figure 4.12:



Figure 4.12: ezAFM Booth at the MRS 2012 Fall Meeting

Also, several visitors had chance to test the ezAFM themselves in this meeting. In Figure 4.13 and Figure 4.14 selected visitor samples from MRS 2012 fall meeting can be seen.

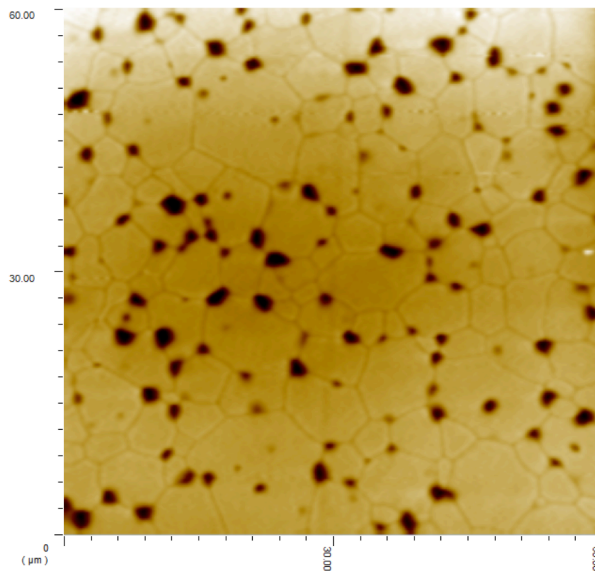


Figure 4.13: Grains in CeO<sub>2</sub> Pellet, sample courtesy of Dr. Claire Corkhill, Sheffield University

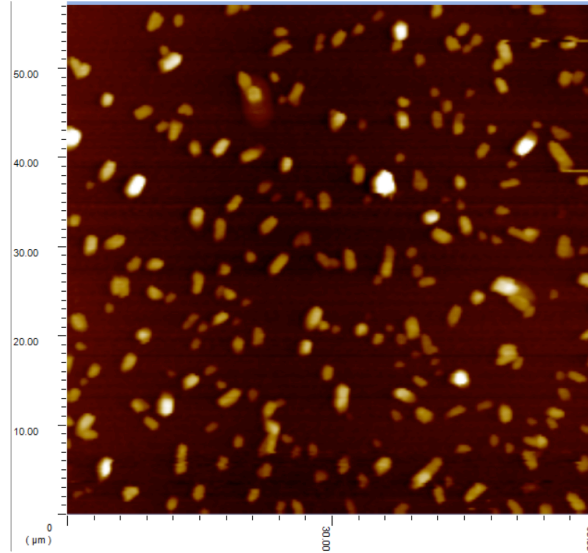


Figure 4.14: Proprietary Crystal Topography – Sample Courtesy of IPG Company

Moreover, ezAFM is demonstrated while imaging human red blood cells to the Minister of Development, Mr. Cevdet Yılmaz, the President of TÜBİTAK, Prof. Dr. Yücel Altunbaşak and President of Sabancı University, Prof. Dr. Nihat Berker during the inauguration of SUNUM laboratories in March 2012.



Figure 4.15: ezAFM presented to the Minister of Development, President of TÜBİTAK and President of Sabancı University while it was imaging human red blood cells

Also ezAFM is invited to a special event as a highly successful SANTEZ project. ezAFM is presented to the Minister of Science, Industry and Technology, Mr. Nihat Ergün in that event.





Figure 4.16: Minister of Science, Industry and Technology and the industrialist Ahmet Nazif Zorlu are inspecting the ezAFM

#### 4.4 Conclusion

In this thesis, a reliable Digital Atomic Force Microscope Control electronics and PC software architecture has been successfully developed and implemented for the ezAFM. The system is based on Xilinx Spartan 3A DSP chip. The main feedback loop runs at 60kHz and uses 24Bit Analog to digital and Digital to Analog Converters. . The cantilever deflection and its phase are measured using a high speed ADC and digital lock in amplifier all implemented in the FPGA. The computer communication is implemented in High Speed USB 2.0 interface.

The ezAFM system runs smoothly on standard samples as it can be seen in the images presented in the previous chapters. Furthermore, it is even capable of imaging atomic steps in Graphite and Gypsum.

The system has been successfully commercialized by the NanoSis and NanoManyetik with the NanoMagnetics Instruments tradename and is being supplied to a number of users worldwide.

## 5 BIBLIOGRAPHY

- [1] G. Binnig and H. Rohrer, "Scanning tunneling microscopy," *Surface Science*, vol. 126, no. 1, pp. 236–244, 1983.
- [2] "Scanning tunneling microscope - Wikipedia, the free encyclopedia." [Online]. Available: [http://en.wikipedia.org/wiki/Scanning\\_tunneling\\_microscope](http://en.wikipedia.org/wiki/Scanning_tunneling_microscope). [Accessed: 25-Jan-2013].
- [3] G. Binnig, C. F. Quate, and C. Gerber, "Atomic force microscope," *Physical review letters*, vol. 56, no. 9, pp. 930–933, 1986.
- [4] "Paul West PHD.com." [Online]. Available: <http://www.paulwestphd.com/book.html>. [Accessed: 25-Jan-2013].
- [5] Y. Martin, C. C. Williams, and H. K. Wickramasinghe, "Atomic force microscope–force mapping and profiling on a sub 100-Å scale," *Journal of Applied Physics*, vol. 61, no. 10, pp. 4723–4729, 1987.
- [6] C. M. Mate, G. M. McClelland, R. Erlandsson, and S. Chiang, "Atomic-scale friction of a tungsten tip on a graphite surface," *Phys. Rev. Lett.*, vol. 59, no. 17, pp. 1942–1945, Oct. 1987.
- [7] O. Marti, J. Colchero, and J. Mlynek, "Combined scanning force and friction microscopy of mica," *Nanotechnology*, vol. 1, no. 2, pp. 141–144, Oct. 1990.
- [8] "Atomic Force Microscopy overview." [Online]. Available: <http://www.nanoscience.com/education/afm.html>. [Accessed: 25-Jan-2013].
- [9] G. Meyer and N. M. Amer, "Optical-beam-deflection atomic force microscopy: The NaCl (001) surface," *Applied Physics Letters*, vol. 56, no. 21, pp. 2100–2101, May 1990.
- [10] J. Mertens, M. Álvarez, and J. Tamayo, "Real-time profile of microcantilevers for sensing applications," *Applied Physics Letters*, vol. 87, no. 23, pp. 234102–234102–3, Nov. 2005.
- [11] "The Teaching AFM." [Online]. Available: <http://www.media.mit.edu/nanoscale/courses/AFMsite/>. [Accessed: 25-Jan-2013].
- [12] "DIY scanning tunnelling microscope." [Online]. Available: <http://www.instructables.com/community/DIY-scanning-tunnelling-microscope/>. [Accessed: 25-Jan-2013].
- [13] "AMATEUR STM." [Online]. Available: <http://www.angelfire.com/electronic2/spm/index.html>. [Accessed: 25-Jan-2013].
- [14] "STM - Home." [Online]. Available: <http://www.stm-diy.ch/>. [Accessed: 25-Jan-2013].

- [15] "STM Project - an Amateur Scanning Tunneling Microscope." [Online]. Available: <http://www.e-basteln.de/>. [Accessed: 25-Jan-2013].
- [16] "Nanosurf - Easyscan 2." [Online]. Available: <http://www.nanosurf.com/index.cfm?content=0402>. [Accessed: 25-Jan-2013].
- [17] "AFM Workshop - EDUCATION." [Online]. Available: <http://www.afmworkshop.com/atomic-force-microscope-education.php>. [Accessed: 26-Jan-2013].
- [18] "SPM - Scanning Probe Microscopy - NT-MDT." [Online]. Available: <http://www.ntmdt.com/>. [Accessed: 25-Jan-2013].
- [19] "MicroBlaze Soft Processor." [Online]. Available: <http://www.xilinx.com/tools/microblaze.htm>. [Accessed: 25-Jan-2013].
- [20] H. Poincaré, "The theory of Lorentz and the principle of reaction," *Arch. Néerland. Sci*, vol. 5, pp. 252–278, 1900.
- [21] D. Croft, G. Shedd, and S. Devasia, "Creep, hysteresis, and vibration compensation for piezoactuators: atomic force microscopy application," in *American Control Conference, 2000. Proceedings of the 2000*, 2000, vol. 3, pp. 2123–2128.
- [22] H. Kaizuka and B. Siu, "A simple way to reduce hysteresis and creep when using piezoelectric actuators," *Japanese journal of applied physics*, vol. 27, no. 5, pp. L773–L776, 1988.
- [23] K. K. Leang and S. Devasia, "Feedback-linearized inverse feedforward for creep, hysteresis, and vibration compensation in AFM piezoactuators," *Control Systems Technology, IEEE Transactions on*, vol. 15, no. 5, pp. 927–935, 2007.
- [24] K. K. Leang and S. Devasia, "Design of hysteresis-compensating iterative learning control for piezo-positioners: Application to atomic force microscopes," *Mechatronics*, vol. 16, no. 3, pp. 141–158, 2006.
- [25] G. Meyer and N. M. Amer, "Novel optical approach to atomic force microscopy," *Applied Physics Letters*, vol. 53, no. 12, pp. 1045–1047, Sep. 1988.
- [26] "AN1115 - Implementing Digital Lock-In Amplifiers Using the dsPIC DSC - Application Notes - Details." [Online]. Available: [http://www.microchip.com/stellent/idcplg?IdcService=SS\\_GET\\_PAGE&nodeId=1824&appnote=en532447](http://www.microchip.com/stellent/idcplg?IdcService=SS_GET_PAGE&nodeId=1824&appnote=en532447). [Accessed: 25-Jan-2013].
- [27] J. H. Scofield, "Frequency-domain description of a lock-in amplifier," *American Journal of Physics*, vol. 62, no. 2, pp. 129–132, 1994.
- [28] "Xilinx CORE Generator System." [Online]. Available: <http://www.xilinx.com/tools/coregen.htm>. [Accessed: 25-Jan-2013].
- [29] M. J. Humphry, R. Chettle, P. J. Moriarty, M. D. Upward, and P. H. Beton, "Digital scanning probe microscope controller for molecular manipulation applications," *Review of Scientific Instruments*, vol. 71, no. 4, pp. 1698–1701, Apr. 2000.
- [30] B. A. Morgan and G. W. Stupian, "Digital feedback control loops for scanning tunneling microscopes," *Review of Scientific Instruments*, vol. 62, no. 12, pp. 3112–3113, Dec. 1991.
- [31] S. M. Clark, D. R. Baselt, C. F. Spence, M. G. Youngquist, and J. D. Baldeschwieler, "Hardware for digitally controlled scanned probe microscopes," *Review of Scientific Instruments*, vol. 63, no. 10, pp. 4296–4307, Oct. 1992.



- [32] U. Celik, K. Celik, H. Aslan, I. Kehribar, M. Dede, H. O. Ozer, and A. Oral, "ezAFM: A low cost Atomic Force Microscope(AFM)," in *Bulletin of the American Physical Society*, 2012, vol. Volume 57, Number 1.